Range-separated local hybrids

Robin Haunschild, and Gustavo E. Scuseria

View Online   Export Citation

ARTICLES YOU MAY BE INTERESTED IN

Range-separated local hybrids

Robin Haunschild[1,a)] and Gustavo E. Scuseria[1,2]

[1]*Department of Chemistry, Rice University, Houston, Texas 77005, USA*
[2]*Department of Physics and Astronomy, Rice University, Houston, Texas 77005, USA*

We present two range-separated (screened and long-range-corrected) extensions to our recent work on local hybrids of generalized gradient approximation exchange. Our screened local hybrid improves over HSE06 for thermochemistry and barrier heights. The long-range-corrected (LC) local hybrid improves over LC-ωPBE for heats of formation and nonhydrogen transfer reaction barriers but does not reach the accuracy of LC-ωPBE for hydrogen transfer barrier heights. © 2010 American Institute of Physics. [doi:10.1063/1.3451078]

I. INTRODUCTION

Present day applied electronic structure theory is dominated by the Kohn–Sham (KS) density functional theory (DFT).[1–4] The crucial part which determines the accuracy of DFT is the approximation of the exchange-correlation (XC) functional. The simplest approximation to the XC energy density $e_{XC}(\mathbf{r})$ is the local spin density approximation (LSDA),[5,6] where $e_{XC}(\mathbf{r})$ depends on the local density $\rho(\mathbf{r})$. The generalized gradient approximations (GGAs) also incorporate the gradient of the local density ($\nabla\rho$), and the meta-GGA functionals include additional information from the Laplacian of the local density ($\nabla^2\rho$) and/or the noninteracting kinetic energy density (τ), which is expressed in terms of the occupied KS orbitals (ϕ),[7,8]

$$\tau(\mathbf{r}) = \frac{1}{2}\sum_i |\nabla\phi_i(\mathbf{r})|^2. \tag{1}$$

Throughout this paper quantities such as $\rho(\mathbf{r})$, $\nabla\rho$, $\nabla^2\rho$, τ, and ϕ are assumed to be either spin-up or spin-down, but we will suppress the spin indices for conciseness.

Global hybrid[9] functionals incorporating a constant fraction ζ of nonlocal Hartree–Fock-type (HF-type) exchange,

$$E_{XC}^{Gh} = \zeta E_X^{HF} + (1-\zeta)E_X^{DFA} + E_C^{DFA}$$
$$= (E_X^{DFA} - E_X^{HF})(1-\zeta) + E_X^{HF} + E_C^{DFA}, \tag{2}$$

improve the accuracy of DFT for chemical problems significantly and thus have become the method of choice in computational quantum chemistry. In Eq. (2) E_X^{HF} is the HF exchange energy and E_X^{DFA} and E_C^{DFA} are the exchange and correlation energies obtained by a semilocal (LSDA, GGA, or meta-GGA) density functional approximation (DFA). Admixture of a fraction of HF exchange into the XC functional simulates some nondynamical correlation effects,[10–17] and is formally justified by adiabatic connection arguments.[9,18] No constant fraction of HF exchange is found to be the optimum

for all properties.[19] Less HF exchange (about 10%–25%) is desirable for thermochemistry and more HF exchange (around 50% or even more) is favorable for barrier heights.[20,21] Additionally, the optimum amount of HF exchange varies with the hybridized DFA.[22]

One possible solution to this problem are local hybrid functionals,[21,23–31] which employ a position-dependent fraction $f(\mathbf{r})$ of HF exchange,[23,32]

$$E_{XC}^{Lh} = \int [f(\mathbf{r})e_X^{HF}(\mathbf{r}) + [1-f(\mathbf{r})]e_X^{DFA}(\mathbf{r})]d^3\mathbf{r} + E_C^{DFA}$$
$$= \int [e_X^{DFA}(\mathbf{r}) - e_X^{HF}(\mathbf{r})][1-f(\mathbf{r})]d^3\mathbf{r} + E_X^{HF} + E_C^{DFA}. \tag{3}$$

In Eq. (3) $e_X^{DFA}(\mathbf{r})$ is calculated by a semilocal DFA, and the HF exchange energy density $e_X^{HF}(\mathbf{r})$ in the conventional gauge[32–34]

$$e_X^{HF}(\mathbf{r}) = -\frac{1}{2}\sum_{i,j} \phi_i^*(\mathbf{r})\phi_j(\mathbf{r}) \int \frac{\phi_j^*(\mathbf{r}')\phi_i(\mathbf{r}')}{|\mathbf{r}-\mathbf{r}'|}d^3\mathbf{r}' \tag{4}$$

is given in terms of the occupied KS or generalized Kohn–Sham (GKS) orbitals. Jaramillo *et al.*[23] reported the first implementation of the local hybrid ansatz in 2003 with the nonempirical local hybrid mixing function (LMF),

$$f(\mathbf{r}) = \frac{\tau_W(\mathbf{r})}{\tau(\mathbf{r})}, \quad \tau_W(\mathbf{r}) \equiv \frac{|\nabla\rho(\mathbf{r})|^2}{8\rho(\mathbf{r})}, \tag{5}$$

hybridizing B88 (Becke)[35,36] and Perdew–Burke–Ernzerhof[37] (PBE) exchange. This mixing function incorporates no HF exchange in regions of constant density, including the uniform electron gas where semilocal exchange is exact. It admixes 100% HF exchange in one-electron regions, where HF exchange is the exact XC functional. Although this local hybrid showed rather poor thermochemistry results, very promising barrier heights and dissociation behavior of two-center three-electron bonds were obtained.

Later, Kaupp *et al.*[21,24,25] reported that parametrized LMFs including

---

a)Author to whom correspondence should be addressed. Electronic mail: rh8@rice.edu.

$$f(\mathbf{r}) = \alpha_1 \frac{\tau_W(\mathbf{r})}{\tau(\mathbf{r})}, \tag{6}$$

$$f(\mathbf{r}) = \left(\frac{s}{\alpha_2 + s} \right)^2,$$

$$s(\mathbf{r}) = \frac{|\nabla \rho(\mathbf{r})|}{2(3\pi^2)^{1/3} \rho^{4/3}(\mathbf{r})}, \tag{7}$$

and

$$f(\mathbf{r}) = \mathrm{erf}(\alpha_3 s), \tag{8}$$

(where α_1, α_2, and α_3 are empirical parameters) hybridizing LSDA exchange can provide accurate thermochemistry and reaction barriers. The use of a density matrix similarity metric[26,27] has also shown promise for local hybrids of LSDA and GGA exchange. Perdew and co-workers[28] proposed the competitive local hybrid ("hyper-GGA") Perdew–Staroverov–Tao–Scuseria (PSTS) for barrier heights and thermochemistry by hybridizing the meta-GGA Tao–Perdew–Staroverov–Scuseria[38] (TPSS) with HF exchange using five empirical parameters. PSTS is an improvement over TPSS for thermochemistry and barrier heights, but inferior for thermochemistry compared to its "parent" TPSSh (Ref. [39]) (10% HF with 90% TPSS exchange) functional.

Local hybrid functionals were implemented self-consistently within the localized HF/common energy denominator approximation to optimized effective potential by Arbuznikov *et al.*[40] in 2006. This self-consistent localized local hybrid (LLH) method was later extended and applied in calculations of nuclear shielding constants.[41] The implementation is computationally demanding, requiring two separate resolutions of the identity to construct the averaged local potential entering the LLH equations. Most subsequent thermochemical tests of local hybrids have been performed non-self-consistently.[21,24–27,31,42] Self-consistent local hybrids were also implemented within the GKS scheme,[29] which requires just one resolution of the identity and is computationally more tractable. Arbuznikov and co-workers[31] extended the LMFs in Eq. (6) and (8) by an explicit dependence on the spin polarization yielding LMFs with two empirical parameters. They reported a slightly higher accuracy for atomization energies on average thereby sacrificing accuracy for barrier heights, especially for hydrogen transfer reactions.

Recently, we proposed self-consistent local hybrids of GGA exchange (Lh*n*-PBE) (Ref. [30]) within the GKS scheme. They are designed to be small perturbations to the parent global hybrid PBEh (Ref. [43]) (25% HF with 75% PBE exchange). Improvements to atomization energies and barrier heights showed promise for the concept of constructing the LMF of nuclei-centered Gaussian-type contributions on top of a well performing global hybrid introducing only one adjustable parameter.

Range-separated functionals[44–59] represent another possibility to overcome the limitations of global hybrids. They separate the electron-electron interaction operator into at least two components, short-range (SR) and long-range (LR) parts, and treat each part differently,

$$\frac{1}{|\mathbf{r} - \mathbf{r}'|} = \underbrace{\frac{\mathrm{erfc}(\omega|\mathbf{r} - \mathbf{r}'|)}{|\mathbf{r} - \mathbf{r}'|}}_{\mathrm{SR}} + \underbrace{\frac{\mathrm{erf}(\omega|\mathbf{r} - \mathbf{r}'|)}{|\mathbf{r} - \mathbf{r}'|}}_{\mathrm{LR}}. \tag{9}$$

The standard error function, $\mathrm{erf}(x)$, and its complement, $\mathrm{erfc}(x) = 1 - \mathrm{erf}(x)$, are generally chosen for computational convenience. The very accurate LR-corrected LC-ωPBE (Ref. [47]) functional handles the LR exchange interaction with the HF theory and the SR interaction with semilocal DFT, PBE, leaving the correlation functional unseparated,

$$E_{\mathrm{XC}}^{\mathrm{LC}\text{-}\omega\mathrm{PBE}} = E_{\mathrm{X}}^{\mathrm{SR}\text{-}\mathrm{PBE}} + E_{\mathrm{X}}^{\mathrm{LR}\text{-}\mathrm{HF}} + E_{\mathrm{C}}^{\mathrm{PBE}}. \tag{10}$$

The screened Heyd–Scuseria–Ernzerhof (HSE) functional[50] represents the other limiting case. It admixes 25% HF exchange with 75% PBE exchange to describe the SR interaction whereas it employs only PBE exchange in the LR. HSE was designed with solids in mind where LR HF exchange becomes pathological as the band gap closes. HSE has shown to be extremely successful in predicting band gaps and other properties of solids.[60]

On the other hand, the Henderson–Izmaylov–Scuseria–Savin[61,62] functional separates the electron-electron interaction operator in three parts and introduces a middle range (MR). It uses only PBE exchange in the SR and LR with 60% HF exchange and 40% PBE exchange in the MR. Screened as well as LR-corrected functionals of LSDA exchange were locally hybridized with the LMF in Eq. (6) in the SR yielding ωLh-LSDA (Ref. [63]) and LC-Lh-LSDA.[29] The importance of SR HF exchange for core excitations was pointed out recently.[64] Other promising range-separated methods have recently been reported.[65]

Functionals with a constant range-separation parameter ω have obvious limitations. Krukau *et al.*[58] extended the concept to locally range-separated (LRS) functionals with a position-dependent $\omega(\mathbf{r})$. The proposed LRS-ωLSDA functional outperforms its parent LC-ωLSDA for thermochemistry and kinetics.

In this work, we report the introduction of range-separation in our recent Lh3-PBE (Ref. [30]) functional. We will point out here its merits and shortcomings for thermochemistry and kinetics of main group compounds. In the next section, we review briefly the LMF of Lh3-PBE and describe the range separation used in this paper. In Sec. III the details about our calculations are presented. Section IV compares the performance of our new range-separated local hybrids to selected previously reported full-range and range-separated local and global hybrids. Finally, our conclusions are presented in Sec. V.

II. THEORY

The basic ideas of Lh3-PBE are as follows.

- Most properties of chemical significance are improved by a constant admixture of HF exchange.

- Existing semilocal approximations for exchange are generally constructed as expansions around slowly varying densities.

- Semilocal DFAs and global hybrids fail[49,51,52,66,67] when density tail regions are important because they exhibit an XC potential with wrong decay.[68,69]

- Examination of other existing successful LMFs (Refs. 21 and 24–27) shows that they typically include large amounts of HF exchange near nuclei and in stretched-bond situations.

The LMF of Lh3-PBE based upon these ideas is heuristically given by Eq. (11),

$$f(\mathbf{r}) = \zeta + (1 - \zeta)\mathrm{erf}\left(\mathrm{erf}(s)\sum_A e^{-\gamma\tau|\mathbf{r}_A|^2}\right), \quad (11)$$

with

$$s(\mathbf{r}) = \frac{|\nabla\rho(\mathbf{r})|}{2(3\pi^2)^{1/3}\rho^{4/3}(\mathbf{r})}$$

and

$$\tau(\mathbf{r}) = \frac{1}{2}\sum_i |\nabla\phi_i(\mathbf{r})|^2,$$

where ζ and γ are positive parameters, $|\mathbf{r}_A|$ is the distance of the reference point to the nucleus A, and the sum loops over all nuclei A. This local mixing function $f(\mathbf{r})$ has very narrow maxima around nuclei heavier than He. It decays quickly to the base amount ζ between nuclei for equilibrium bond distances but increases to higher values for stretched-bond situations. Asymptotically, far from the nuclei $f(\mathbf{r})$ goes essentially to 1.0 for triatomics and larger molecules.[30] We present LR-corrected

$$E_{\mathrm{XC}}^{\mathrm{LC\text{-}Lh\text{-}PBE}} = \int [e_{\mathrm{X}}^{\mathrm{SR\text{-}PBE}}(\mathbf{r}) - e_{\mathrm{X}}^{\mathrm{SR\text{-}HF}}(\mathbf{r})]$$
$$\times [1 - f(\mathbf{r})]d^3\mathbf{r} + E_{\mathrm{X}}^{\mathrm{HF}} + E_{\mathrm{C}}^{\mathrm{PBE}} \quad (12)$$

and screened variants of Lh3-PBE

$$E_{\mathrm{XC}}^{\omega\mathrm{Lh\text{-}PBE}} = \int [e_{\mathrm{X}}^{\mathrm{SR\text{-}PBE}}(\mathbf{r}) - e_{\mathrm{X}}^{\mathrm{SR\text{-}HF}}(\mathbf{r})]$$
$$\times [1 - f(\mathbf{r})]d^3\mathbf{r} + E_{\mathrm{X}}^{\mathrm{SR\text{-}HF}} + E_{\mathrm{X}}^{\mathrm{LR\text{-}PBE}} + E_{\mathrm{C}}^{\mathrm{PBE}}. \quad (13)$$

In both cases the local hybridization is done only for the SR exchange interaction. In the limit $\omega\to\infty$, ωLh-PBE reduces to pure PBE and LC-Lh-PBE becomes identical with HF exchange with PBE correlation. The other limiting case ($\omega\to0$) recovers Lh3-PBE with different values of ζ and/or γ for both types of range-separated local hybrids.

We have performed free and constraint optimizations to determine the values of the parameters ζ, γ, and ω. Adjustable parameters are fitted within the AE6 (six atomization energies) and BH6 (three forward and reverse hydrogen transfer barrier heights) test sets[70] to minimize the average mean absolute error (AMAE) which is only intended to be used within the optimization process and not as a quality criterion for the given density functional,
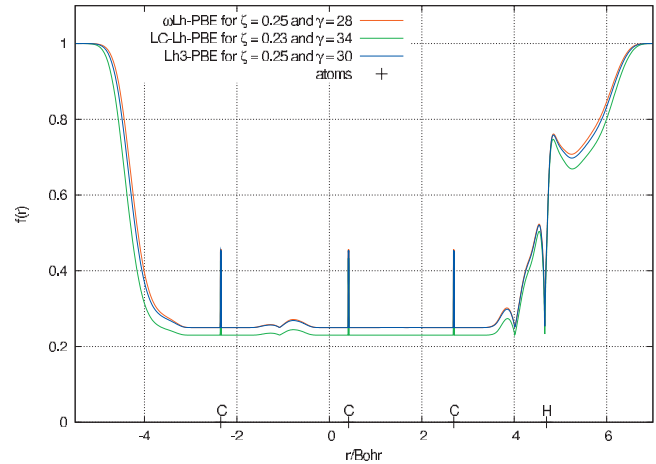

FIG. 1. The local mixing function for propyne along the linear C–C–C–H axis looks similar for all presented cases [ωLh-PBE (red line), LC-Lh-PBE (green line), and Lh3-PBE (blue line)].

$$\mathrm{AMAE} = \frac{\mathrm{MAE(AE6)} + \mathrm{MAE(BH6)}}{2}. \quad (14)$$

For the screened local hybrid we have imposed the constraint $\omega = \omega_{\mathrm{HSE06}} = 0.11a_0^{-1}$.[71] Additionally to free parametrizations to the fitting test set, we also performed constrained optimizations of the adjustable parameters by requiring $\zeta = \zeta_{\mathrm{PBEh}} = 0.25$ for both range-separated local hybrids.[72] Due to the small fitting test set with 12 reference values, we performed calculations for all local minima in parameter space in our larger verification test sets (see Secs. III and IV) and pick the parameter sets with the best overall performance. The screened local hybrid does not benefit from relaxation of ζ whereas the LR-corrected local hybrid does. Our recommended parameter values are as follows:

- ωLh-PBE: $\zeta = 0.25$, $\gamma = 28$, and $\omega = 0.11a_0^{-1}$ and

- LC-Lh-PBE: $\zeta = 0.23$, $\gamma = 34$, and $\omega = 0.16a_0^{-1}$.

Thus, our screened local hybrid contains two empirical parameters (γ and ω) adding only one adjustable parameter to HSE06.[45,71,73] Our LR-corrected local hybrid, on the other hand, contains three adjustable parameters.

More details on calculations with other than our recommended parameter values are discussed in Sec. IV. The LMFs for both cases look similar to each other and to that of Lh3-PBE, as shown in Fig. 1 for propyne as an example. The amount of admixed HF exchange around the bond midpoint increases with larger N–N distance, as shown in Fig. 2 for N_2 where the LMFs of LC-Lh-PBE and LC-Lh-LSDA (Refs. 29 and 63) are presented at four different N–N distances. The dependence of the MAE on the precise values of the parameters is rather small, as shown in Fig. 3. The optimum values of ζ and ω for LC-Lh-PBE are determined by both the AE6 and BH6 test sets. Note that ζ and ω were not fitted for the recommended parameter set of ωLh-PBE. The MAE of the BH6 test set is virtually independent of γ within the shown range for both LC-Lh-PBE and ωLh-PBE. Thus, the opti-

(a) equilibrium distance (approx. 2.076 Bohr)

(b) r(N-N) = 2 Å (approx. 3.780 Bohr)

(c) r(N-N) = 3 Å (approx. 5.669 Bohr)

(d) r(N-N) = 4 Å (approx. 7.559 Bohr)
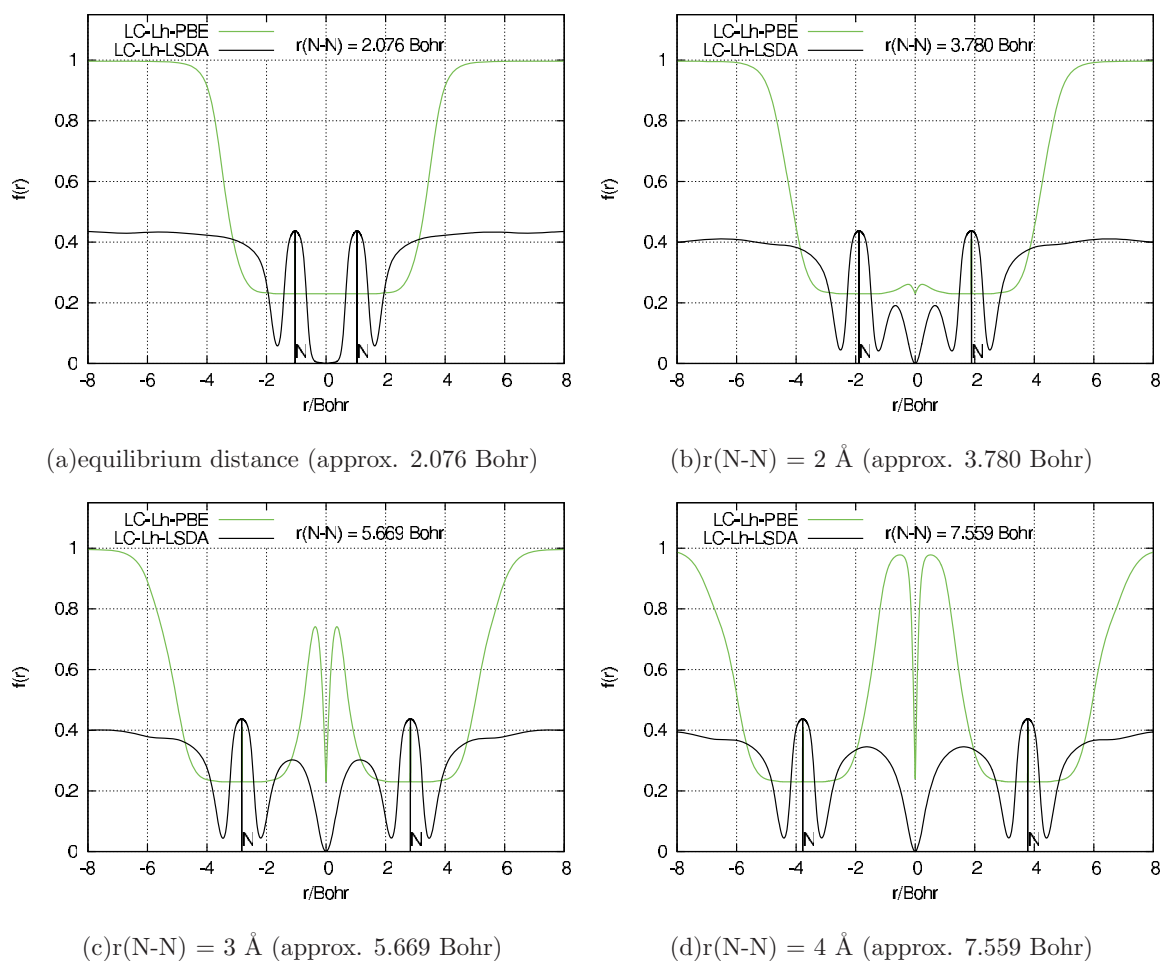
FIG. 2. Local mixing functions for N_2 of LC-Lh-PBE (green line) and LC-Lh-LSDA (black line) for different distances.

mum value of γ is determined by the MAE of the AE6 test set only. The implementation of the employed self-consistent algorithm was presented previously.[29]

III. COMPUTATIONAL DETAILS

All calculations were carried out using the development version of the GAUSSIAN electronic structure program.[74] The fully uncontracted 6-311++G(3df,3pd) basis set[75,76] was employed for molecular test set calculations to obtain benchmark quality results. Calculations to compare absolute atomic energies against accurate nonrelativistic reference values[77] used the very large UGBS2P basis set,[78] which is considered to be very close to the basis set limit. For numerical integration of the DFT XC potential, we used the UltraFine grid with 99 radial shells and 590 angular points, except those for the plots of the local mixing functions and atomic energy calculations, where a grid of 999 radial shells and 590 angular points was used. Test calculations for the molecular test sets showed that a grid with more than 99 radial shells does not change the results noticeably. All presented calculations were carried out self-consistently as described in Ref. 29.

The proposed range-separated local hybrids were tested in combination with PBE.[37] The large G3/99 (223 molecules)[79] test set and its subsets G2/97 (148 molecules)[80] and G3-3 (75 molecules)[81] were used to assess the accuracy

for enthalpies of formation. B3LYP/6-31G(2df,p) geometries and zero-point energies with a frequency scale factor of 0.9854 were used, as recommended in Ref. 82. Additionally, we assessed the performance for reaction barrier heights using the HTBH38/04 and NHTBH38/04 test sets[83,84] (19 forward and reverse hydrogen and nonhydrogen transfer barrier heights, respectively). The molecular geometries of the AE6, BH6, HTBH38/04, and NHTBH38/04 test sets are evaluated at the QCISD/MG3 level of theory.[85–88]

The proposed local hybrid functionals are compared to B3LYP,[11,35,36] PBEh,[43,89] TPSSh,[39] HSE06,[45,71,73] LC-ωPBE,[47] and Lh-LSDA ($c=0.48$; also referred to as t-LMF in Refs. 24, 21, and 30),

$$f(\mathbf{r}) = c \frac{\tau_W}{\tau}, \tag{15}$$

hybridizing LSDA,[5,6] and its range-separated variants ωLh-LSDA ($c=0.55$ and $\omega=0.11a_0^{-1}$) (Refs. 29 and 63) and LC-Lh-LSDA ($c=0.44$ and $\omega=0.18a_0^{-1}$).[29]

Calculations of open-shell species were carried out spin unrestricted. All used geometries, zero-point energies, and reference values are available from Refs. 30 and 78. Errors are reported as *calculated-reference*.
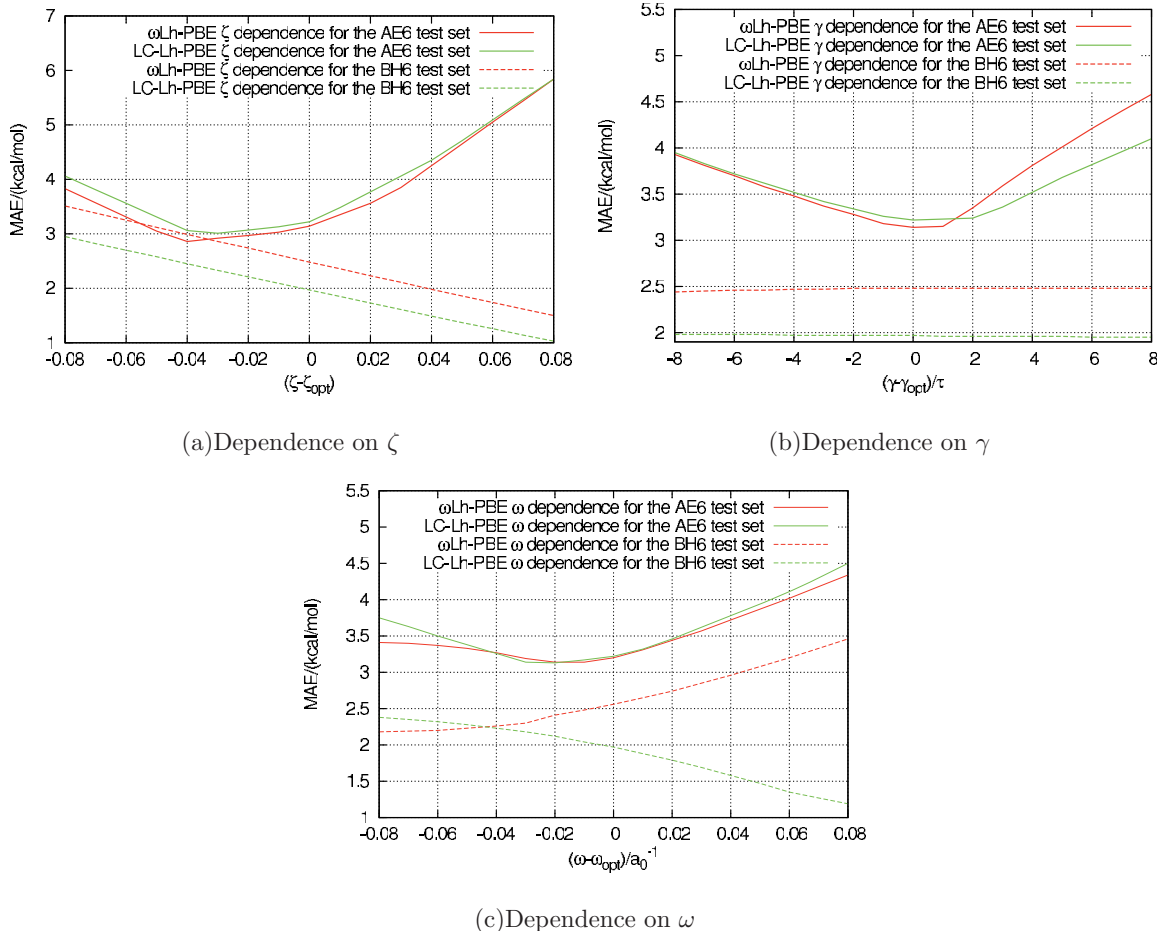
(a)Dependence on ζ

(b)Dependence on γ

(c)Dependence on ω

FIG. 3. Dependence of the MAE on the parameters for ωLh-PBE (red lines) and LC-Lh-PBE (green lines).

IV. RESULTS

According to the AE6 and BH6 test sets which were used to fit the adjustable parameters, Lh3-PBE, LC-Lh-PBE, and ωLh-PBE have similar accuracy for atomization energies although LC-Lh-PBE is more accurate for barrier heights, as shown in Table I. A change of ω for ωLh-PBE showed only very small effects within the fitting test set: Atomization energies worsen slightly and barrier heights improve somewhat [Fig. 3(c)], overall yielding essentially the same AMAE. We also tried to optimize ζ for ωLh-PBE which yielded a lower AMAE for ωLh-PBE but somewhat worse overall performance in larger test sets (G3/99, HTBH38/04, and NHTBH38/04), which is a sign of overparametrization to the fitting test set and thereby losing universal applicability.

TABLE I. Mean errors (MEs) and MAEs for the AE6 and BH6 test sets in kcal/mol.

	AE6		BH6	
	ME	MAE	ME	MAE
PBEh	0.3	6.2	−4.9	4.9
Lh3-PBE	−2.4	3.1	−2.3	2.3
ωLh-PBE	−2.7	3.1	−2.5	2.5
LC-Lh-PBE	−2.8	3.2	−2.0	2.0

We found the following minima in parameter space for LC-Lh-PBE:

(a) $\zeta=0.23$, $\gamma=34$, and $\omega=0.16a_0^{-1}$,
(b) $\zeta=0.09$, $\gamma=60$, and $\omega=0.33a_0^{-1}$, and
(c) $\zeta=0.25$, $\gamma=33$, and $\omega=0.14a_0^{-1}$.

We recommend to use the parameter set (a). The two parameter sets (b) and (c) yield rather large MAE values for the G3-3 test set. Parameter set (b) yields lower MAE values for barrier heights (1.4 kcal/mol for HTBH38/04 and 1.7 kcal/mol for NHTBH38/04) but rather high MAE values for heats of formation (3.4 kcal/mol for G2/97, 5.0 kcal/mol for G3-3, and 3.9 kcal/mol for G3/99). The parameter set (c) was reached by imposing the constraint $\zeta=\zeta(\text{PBEh})=0.25$ on LC-Lh-PBE while adjusting γ and ω. Its parameter values are close to those of our recommended set of parameters. Both the MAEs of the AE6 and the BH6 test sets increase slightly due to the constraint $\zeta=\zeta(\text{PBEh})=0.25$. The impact on larger barrier height test sets are minor but the MAE for the G3-3 test set is 0.5 kcal/mol higher due to this constraint on ζ. Therefore, we reject the parameter sets (b) and (c) in the following and continue to discuss only the results obtained with the recommended parameter values.

The screened local hybrid ωLh-PBE performs slightly better for heats of formation ($\Delta_f H_{298}^\circ$, Ref. 90) than its LR-corrected counterpart LC-Lh-PBE, as shown in Table II.
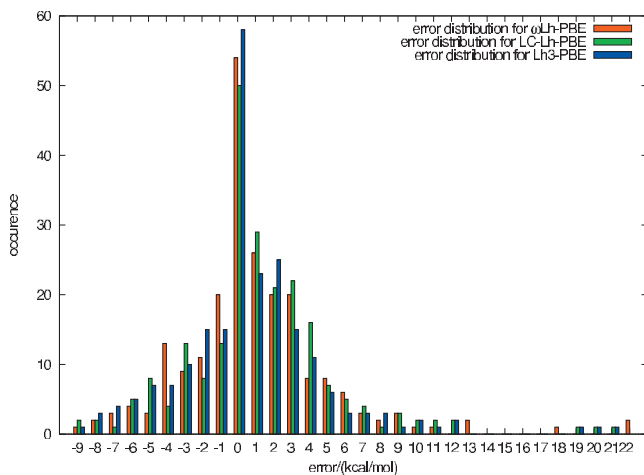
TABLE II. MEs and MAEs for standard enthalpies of formation ($\Delta_f H^\circ_{298}$) of the G2/97, G3-3, and G3/99 test sets in kcal/mol.

	G2/97		G3-3		G3/99	
	ME	MAE	ME	MAE	ME	MAE
PBEh	−2.6	5.0	−9.6	10.4	−4.9	6.8
Lh3-PBE	0.5	3.0	1.2	3.7	0.8	3.2
ωLh-PBE	0.7	3.0	1.6	3.7	1.0	3.3
LC-Lh-PBE	0.9	3.1	2.0	4.1	1.3	3.4
Lh-LSDA[a,b]	−2.5	4.2	−1.2	3.3	−2.1	3.9
ωLh-LSDA	1.2	4.3	6.2	6.6	2.9	5.0
LC-Lh-LSDA	−1.7	3.9	1.8	3.8	−0.5	3.9
HSE06	−1.0	4.0	−5.3	7.0	−2.5	5.0
LC-ωPBE[a]	−0.4	3.9	−2.0	5.2	−0.9	4.3
B3LYP	0.9	3.1	7.9	8.2	3.3	4.8
TPSSh	−1.9	4.4	−1.0	3.5	−1.6	4.1

[a]Reference 91.
[b]Reference 92.

This is mainly due to the G3-3 subset as the MAE values for the G2/97 subset are very similar. The MAE values for the G2/97, G3-3, and G3/99 test sets of ωLh-PBE are very similar to those of Lh3-PBE, as expected: The SR interaction is not that short ranged with $\omega=0.11a_0^{-1}$. Compared to HSE06, ωLh-PBE is a significant improvement for heats of formation: The MAE of ωLh-PBE is 1 kcal/mol lower for the G2/97 test set than that of HSE06 and the G3-3 test set error is nearly halved obtaining a lower MAE in the full G3/99 test set by 2.7 kcal/mol. The improvements over ωLh-LSDA are on a similar scale, as ωLh-LSDA yields quite similar MAE values compared to HSE06.

LC-Lh-PBE performs better in the G2/97 subset and slightly worse in the G3-3 subset than LC-Lh-LSDA, yielding an overall improvement for the full G3/99 test set of 0.5 kcal/mol. It improves over LC-ωPBE in all three heat of formation test sets. ωLh-PBE, LC-Lh-PBE, and their full-range complement have a very similar error distribution within the G3/99 test set, as shown in Fig. 4. Both range-separated local hybrids and Lh3-PBE have in common that they show a few outliers (18 and 22 kcal/mol for ωLh-PBE and 19, 20, and 21 kcal/mol for LC-Lh-PBE and Lh3-PBE).

For all three functionals, the outliers are PF_5, SF_6, and SiF_4. The origin of these exceptional large errors has been discussed previously.[30] The bulk of the error distribution is between −5 and 6 kcal/mol.

The proposed range-separated local hybrids improve over all considered DFAs but LC-ωPBE, TPSSh, and B3LYP for absolute atomic energies, as shown in Table III. The lowest mean absolute error per electron (MAEPE) is obtained with TPSSh. Interestingly, TPSSh and B3LYP are the only DFAs considered in this study which overestimate the absolute total energy of all atoms H–Ar, i.e., yield only negative errors. Lh-LSDA underestimates all considered absolute atomic total energies, thereby yielding only positive errors. PBEh and HSE06 underestimate all absolute total energies but that of the hydrogen atom. ωLh-LSDA overestimates only the absolute total energy of the helium atom and Lh3-PBE, ωLh-PBE, LC-Lh-PBE, LC-Lh-LSDA, and LC-ωPBE underestimate the absolute total energy of all atoms but hydrogen and helium.

ωLh-PBE performs somewhat worse for reaction barrier heights than Lh3-PBE, LC-Lh-PBE, Lh-LSDA, ωLh-LSDA, LC-Lh-LSDA, and LC-ωPBE but improves over its parent HSE06 and commonly employed global hybrids such as PBEh, TPSSh, and B3LYP, as shown in Table IV. All full-

FIG. 4. Error distribution (rounded down errors) within the G3/99 test set for ωLh-PBE (red bars), LC-Lh-PBE (green bars), and Lh3-PBE (blue bars).

TABLE III. MEs, MAEs, and MAEPEs for absolute atomic energies for H–Ar in mhartree.

	ME	MAE	MAEPE
PBEh	66.2	66.3	6.3
Lh3-PBE	58.0	58.8	5.5
ωLh-PBE	48.5	49.4	4.7
LC-Lh-PBE	45.7	46.7	4.4
Lh-LSDA	361.1	361.1	29.8
ωLh-LSDA	317.1	317.4	25.8
LC-Lh-LSDA	356.1	356.8	29.4
HSE06	56.2	56.3	5.4
LC-ωPBE	43.8	44.6	4.2
TPSSh	−24.7	24.7	2.6
B3LYP	−29.2	29.2	3.3

TABLE IV. MEs and MAEs for hydrogen transfer barrier height (HTBH38/04) and nonhydrogen transfer barrier height (NHTBH38/04) test sets in kcal/mol.

	HTBH38/04		NHTBH38/04	
	ME	MAE	ME	MAE
PBEh	−4.7	4.7	−3.2	3.7
Lh3-PBE	−1.9	2.4	−1.9	2.5
ωLh-PBE	−2.1	2.6	−2.4	3.0
LC-Lh-PBE	−1.5	2.1	−1.1	1.8
Lh-LSDA[a]	−2.5	2.8	−1.9	2.5
ωLh-LSDA [a]	−1.6	2.2	−1.5	2.1
LC-Lh-LSDA[a]	−1.9	2.4	−0.8	2.1
HSE06[a]	−4.7	4.7	−3.5	3.9
LC-ωPBE [a]	−0.5	1.3	1.4	2.4
TPSSh	−6.4	6.4	−6.9	7.0
B3LYP	−4.5	4.6	−4.6	4.7

[a]Reference 92.

range and range-separated local hybrids outperform any global hybrid in Table IV. LC-Lh-PBE improves on average over all DFAs in Table IV but LC-ωPBE. It performs quite similar to ωLh-LSDA for kinetics although we would have expected a performance more like LC-Lh-LSDA, as both (LC-Lh-PBE and LC-Lh-LSDA) are LR-corrected versions of well performing local hybrids. LC-Lh-PBE has a more uniform performance for barrier heights than LC-ωPBE, thereby improving over LC-ωPBE for nonhydrogen transfer barrier heights but sacrificing some accuracy for hydrogen transfer barrier heights.

V. CONCLUSIONS

We have extended our recent local hybrid Lh3-PBE (perturbation to PBEh)[30] with range-separation yielding a screened (ωLh-PBE) and a LR-corrected (LC-Lh-PBE) variant of Lh3-PBE. These range-separated local hybrids are best seen as a perturbation to Lh3-PBE because the employed values of the range-separation parameter ω are rather small. Also our recommended parameter sets vary only slightly from that of Lh3-PBE. ωLh-PBE has two empirical parameters and LC-Lh-PBE has three of them.

ωLh-PBE retains the performance of Lh3-PBE for heats of formation but sacrifices some accuracy for reaction barriers. The advantage of ωLh-PBE over Lh3-PBE is that it can be used efficiently for extended systems because we adopted the screening parameter from HSE06. It is encouraging that ωLh-PBE improves over HSE06 for thermochemistry and reaction barriers.

LC-Lh-PBE improves over Lh3-PBE noticeably for barrier height calculations, thereby performing slightly less well than Lh3-PBE for heats of formation. It improves over LC-ωPBE for heats of formation and nonhydrogen transfer barrier heights but does not reach the accuracy of LC-ωPBE for hydrogen transfer reaction barriers.

ACKNOWLEDGMENTS

[1] P. Hohenberg and W. Kohn, Phys. Rev. **136**, B864 (1964).
[2] W. Kohn and L. J. Sham, Phys. Rev. **140**, A1133 (1965).
[3] R. G. Parr and W. Yang, *Density-Functional Theory of Atoms and Molecules* (Oxford University Press, New York, 1989).
[4] W. Koch and M. C. Holthausen, *A Chemist's Guide to Density Functional Theory* (Wiley-VCH, Weinheim, 2001).
[5] J. C. Slater, Phys. Rev. **81**, 385 (1951).
[6] S. H. Vosko, L. Wilk, and M. Nusair, Can. J. Phys. **58**, 1200 (1980).
[7] J. P. Perdew and K. Schmidt, in *Density Functional Theory and its Application to Materials*, edited by V. Van Doren, C. Van Alsenoy, and P. Geerlings (American Institute of Physics, Melville, NY, 2001).
[8] G. E. Scuseria and V. N. Staroverov, in *Theory and Applications of Computational Chemistry: The First 40 Years*, edited by C. E. Dykstra, G. Frenking, K. S. Kim, and G. E. Scuseria (Elsevier, Amsterdam, 2005).
[9] A. D. Becke, J. Chem. Phys. **98**, 1372 (1993).
[10] A. D. Becke, J. Chem. Phys. **98**, 5648 (1993).
[11] P. J. Stephens, F. J. Devlin, C. F. Chabalowski, and M. J. Frisch, J. Phys. Chem. **98**, 11623 (1994).
[12] O. V. Gritsenko, P. R. T. Schipper, and E. J. Baerends, J. Chem. Phys. **107**, 5007 (1997).
[13] A. D. Becke, J. Chem. Phys. **112**, 4020 (2000).
[14] D. Cremer, Mol. Phys. **99**, 1899 (2001).
[15] E. J. Baerends and O. V. Gritsenko, J. Chem. Phys. **123**, 062202 (2005).
[16] A. D. Becke, J. Chem. Phys. **119**, 2972 (2003).
[17] A. D. Becke, J. Chem. Phys. **122**, 064101 (2005).
[18] W. Yang, J. Chem. Phys. **109**, 10107 (1998).
[19] K. Burke, M. Ernzerhof, and J. P. Perdew, Chem. Phys. Lett. **265**, 115 (1997).
[20] J. L. Durant, Chem. Phys. Lett. **256**, 595 (1996).
[21] M. Kaupp, H. Bahmann, and A. V. Arbuznikov, J. Chem. Phys. **127**, 194102 (2007).
[22] H. L. Schmider and A. D. Becke, J. Chem. Phys. **109**, 8188 (1998).
[23] J. Jaramillo, G. E. Scuseria, and M. Ernzerhof, J. Chem. Phys. **118**, 1068 (2003).
[24] H. Bahmann, A. Rodenberg, A. V. Arbuznikov, and M. Kaupp, J. Chem. Phys. **126**, 011103 (2007).
[25] A. V. Arbuznikov and M. Kaupp, Chem. Phys. Lett. **440**, 160 (2007).
[26] B. G. Janesko and G. E. Scuseria, J. Chem. Phys. **127**, 164117 (2007).
[27] B. G. Janesko and G. E. Scuseria, J. Chem. Phys. **128**, 084111 (2008).
[28] J. P. Perdew, V. N. Staroverov, J. Tao, and G. E. Scuseria, Phys. Rev. A **78**, 052513 (2008).
[29] B. G. Janesko, A. V. Krukau, and G. E. Scuseria, J. Chem. Phys. **129**, 124110 (2008).
[30] R. Haunschild, B. G. Janesko, and G. E. Scuseria, J. Chem. Phys. **131**, 154112 (2009).
[31] A. V. Arbuznikov, H. Bahmann, and M. Kaupp, J. Phys. Chem. A **113**, 11898 (2009).
[32] K. Burke, F. G. Cruz, and K.-C. Lam, J. Chem. Phys. **109**, 8161 (1998).
[33] J. Tao, V. N. Staroverov, G. E. Scuseria, and J. P. Perdew, Phys. Rev. A **77**, 012509 (2008).
[34] The discussion of the gauge problem is beyond the scope of our present study and is therefore ignored.
[35] A. D. Becke, Phys. Rev. A **38**, 3098 (1988).
[36] C. Lee, W. Yang, and R. G. Parr, Phys. Rev. B **37**, 785 (1988).
[37] J. P. Perdew, K. Burke, and M. Ernzerhof, Phys. Rev. Lett. **77**, 3865 (1996); **78**, 1396 (1997).
[38] J. Tao, J. P. Perdew, V. N. Staroverov, and G. E. Scuseria, Phys. Rev. Lett. **91**, 146401 (2003).
[39] V. N. Staroverov, G. E. Scuseria, J. Tao, and J. P. Perdew, J. Chem. Phys. **119**, 12129 (2003); **121**, 11508 (2004).
[40] A. V. Arbuznikov, M. Kaupp, and H. Bahmann, J. Chem. Phys. **124**, 204102 (2006).
[41] A. V. Arbuznikov and M. Kaupp, Chem. Phys. Lett. **442**, 496 (2007).
[42] A. V. Arbuznikov and M. Kaupp, J. Chem. Phys. **128**, 214107 (2008).
[43] C. Adamo and V. Barone, J. Chem. Phys. **110**, 6158 (1999).
[44] A. Savin, in *Recent Developments and Applications in Modern Density Functional Theory*, edited by J. M. Seminario (Elsevier, Amsterdam, 1996), pp. 327–357.

[45] J. Heyd and G. E. Scuseria, J. Chem. Phys. **121**, 1187 (2004).

[46] J. Heyd, J. E. Peralta, G. E. Scuseria, and R. L. Martin, J. Chem. Phys. **123**, 174101 (2005).

[47] O. A. Vydrov and G. E. Scuseria, J. Chem. Phys. **125**, 234109 (2006).

[48] M. Ernzerhof and J. P. Perdew, J. Chem. Phys. **109**, 3313 (1998).

[49] H. Iikura, T. Tsuneda, T. Yanai, and K. Hirao, J. Chem. Phys. **115**, 3540 (2001).

[50] J. Heyd, G. E. Scuseria, and M. Ernzerhof, J. Chem. Phys. **118**, 8207 (2003); **124**, 219906 (2006).

[51] Y. Tawada, T. Tsuneda, S. Yanagisawa, T. Yanai, and K. Hirao, J. Chem. Phys. **120**, 8425 (2004).

[52] I. C. Gerber and J. G. Ángyán, Chem. Phys. Lett. **415**, 100 (2005).

[53] M. Kamiya, H. Sekino, T. Tsuneda, and K. Hirao, J. Chem. Phys. **122**, 234111 (2005).

[54] O. A. Vydrov, J. Heyd, A. V. Krukau, and G. E. Scuseria, J. Chem. Phys. **125**, 074106 (2006).

[55] O. A. Vydrov, G. E. Scuseria, and J. P. Perdew, J. Chem. Phys. **126**, 154109 (2007).

[56] E. Livshits and R. Baer, Phys. Chem. Chem. Phys. **9**, 2932 (2007).

[57] T. M. Henderson, B. G. Janesko, and G. E. Scuseria, J. Chem. Phys. **128**, 194105 (2008).

[58] A. V. Krukau, G. E. Scuseria, J. P. Perdew, and A. Savin, J. Chem. Phys. **129**, 124103 (2008).

[59] T. M. Henderson, B. G. Janesko, G. E. Scuseria, and A. Savin, Int. J. Quantum Chem. **109**, 2023 (2009).

[60] B. G. Janesko, T. M. Henderson, and G. E. Scuseria, Phys. Chem. Chem. Phys. **11**, 443 (2009).

[61] T. M. Henderson, A. F. Izmaylov, G. E. Scuseria, and A. Savin, J. Chem. Phys. **127**, 221103 (2007).

[62] T. M. Henderson, A. F. Izmaylov, G. E. Scuseria, and A. Savin, J. Chem. Theory Comput. **4**, 1254 (2008).

[63] ωLh-LSDA is refered to as SC-Lh-LSDA in Ref. 29.

[64] N. A. Besley, M. J. G. Peach, and D. J. Tozer, Phys. Chem. Chem. Phys. **11**, 10350 (2009).

[65] A. Nakata, T. Tsuneda, and K. Hirao, "Modified regional self-interaction correction method based on the pseudospectral method", J. Phys. Chem. A (to be published).

[66] A. Dreuw and M. Head-Gordon, Chem. Rev. (Washington, D.C.) **105**, 4009 (2005).

[67] H. Sekino, Y. Maeda, and M. Kamiya, Mol. Phys. **103**, 2183 (2005).

[68] C. O. Almbladh and A. C. Pedroza, Phys. Rev. A **29**, 2322 (1984).

[69] M. Levy, J. P. Perdew, and V. Sahni, Phys. Rev. A **30**, 2745 (1984).

[70] B. J. Lynch and D. G. Truhlar, J. Phys. Chem. A **107**, 8996 (2003); **108**, 1460 (2004).

[71] A. V. Krukau, O. A. Vydrov, A. F. Izmaylov, and G. E. Scuseria, J. Chem. Phys. **125**, 224106 (2006).

[72] J. P. Perdew, M. Ernzerhof, and K. Burke, J. Chem. Phys. **105**, 9982 (1996).

[73] J. Heyd and G. E. Scuseria, J. Chem. Phys. **120**, 7274 (2004).

[74] M. J. Frisch, G. W. Trucks, H. B. Schlegel *et al.*, GAUSSIAN, Revision G.01, Gaussian, Inc., Wallingford CT, 2007.

[75] A. D. McLean and G. S. Chandler, J. Chem. Phys. **72**, 5639 (1980).

[76] R. Krishnan, J. S. Binkley, R. Seeger, and J. A. Pople, J. Chem. Phys. **72**, 650 (1980).

[77] S. J. Chakravorty, S. R. Gwaltney, E. R. Davidson, F. A. Parpia, and C. F. p Fischer, Phys. Rev. A **47**, 3649 (1993).

[78] E. V. R. de Castro and F. E. Jorge, J. Chem. Phys. **108**, 5225 (1998).

[79] COF_2 was included in the G2/97 and G3/99 test sets following Ref. 39.

[80] L. A. Curtiss, K. Raghavachari, P. C. Redfern, and J. A. Pople, J. Chem. Phys. **106**, 1063 (1997).

[81] L. A. Curtiss, K. Raghavachari, P. C. Redfern, and J. A. Pople, J. Chem. Phys. **112**, 7374 (2000).

[82] L. A. Curtiss, P. C. Redfern, K. Raghavachari, and J. A. Pople, J. Chem. Phys. **114**, 108 (2001).

[83] Y. Zhao, B. J. Lynch, and D. G. Truhlar, J. Phys. Chem. A **108**, 2715 (2004).

[84] Y. Zhao, N. Gónzales-García, and D. G. Truhlar, J. Phys. Chem. A **109**, 2012 (2005); **109**, 4942 (2006).

[85] J. A. Pople, M. Head-Gordon, and K. Raghavachari, J. Chem. Phys. **87**, 5968 (1987).

[86] P. L. Fast, M. L. Sánchez, and D. G. Truhlar, Chem. Phys. Lett. **306**, 407 (1999).

[87] L. A. Curtiss, P. C. Redfern, K. Raghavachari, V. Rassolov, and J. A. Pople, J. Chem. Phys. **110**, 4703 (1999).

[88] L. A. Curtiss, K. Raghavachari, P. C. Redfern, V. Rassolov, and J. A. Pople, J. Chem. Phys. **109**, 7764 (1998).

[89] M. Ernzerhof and G. E. Scuseria, J. Chem. Phys. **110**, 5029 (1999).

[90] Please note that the assessed quantity here is the atomization energy rather than the enthalpy of formation because the thermodynamical corrections were not calculated by these methods but on the B3LYP/6-31G(2df,p) level of theory.

[91] These results differ slightly from those published in Ref. 29 due to the computational setup (we included Si_2 here).

[92] These results differ slightly from those published in Refs. 21, 24, 25, and 29 due to the computational setup (we used GKS calculations with a different basis set).